Uterine PEComas: A Morphological, Immunohistochemical, and Molecular Analysis of 32 Tumors

Jennifer A. Bennett[1], Ana Costa Braga[2], Andre Pinto[3], Koen Van de Vijver[4], Kristine Cornejo[5], Anna Pesci[6], Lei Zhang[7], Vicente Morales-Oyarvide[8], Takako Kiyokawa[9], Gian Franco Zannoni[10], Joseph Carlson[11], Tomas Slavik[12], Carmen Tornos[13], Cristina R. Antonescu[7], Esther Oliva[14]

[1]Lahey Hospital and Medical Center, [2]Hospital Prof. Doutor Fernando Fonseca, [3]University of Miami, [4]Cancer Research Institute Ghent and Ghent University Hospital, [5]University of Massachusetts, [6]Ospedale Sacro Cuore Don Calabria, [7]Memorial Sloan Kettering Cancer Center, [8]Dana Farber Cancer Institute, [9]Jikei University, [10]Catholic University of Sacred Heart, [11]Karolinska Institutet and Karolinska University Hospital, [12]Ampath Pathology Laboratories and University of Pretoria, [13]Stony Brook Medicine, [7]Memorial Sloan Kettering Cancer Center, [14]Massachusetts General Hospital

Running Title: Analysis of Uterine PEComas

Correspondence
Jennifer A. Bennett, MD, University of Chicago Medicine, 5841 S. Maryland Ave MC 6101, Chicago, IL 60637, Email: jabennett@.uchicago.edu

Conflicts of Interest and Source of Funding
The authors have disclosed that they have no significant relationships with, or financial interest in, any commercial companies pertaining to this article. This study was supported by the Vickery Grant from the Massachusetts General Hospital, and in part by P50-CA140146-01 (CRA) and P30-CA008748 (CRA).

ABSTRACT

Uterine perivascular epithelioid cell tumors (PEComas) are rare neoplasms that may show overlapping morphology and immunohistochemistry with uterine smooth muscle tumors. In this study, we evaluated the morphological, immunohistochemical, and molecular features of 32 PEComas, including 11 with aggressive behavior. Two distinct morphologies were observed: classic (n=30) and those with a lymphangioleiomyomatosis appearance (n=2). In the former, patients ranged from 32 to 77 (mean 51) years and 13% had tuberous sclerosis. Tumors ranged from 0.2 to 17 (mean 5.5) cm with 77% arising in the corpus. Epithelioid cells were present in 100% and a spindled component was seen in 37%. Nuclear atypia was low (53%), intermediate (17%), or high (30%). Mitoses ranged from 0-36 (mean 6) and 0-133 (mean 19) per 10 and 50 high-power fields, with atypical mitoses present in 30%. Thin and delicate vessels were noted in 100%, clear/eosinophilic and granular cytoplasm in 93%, stromal hyalinization in 73%, necrosis in 30%, and lymphovascular invasion in 10%. All tumors were positive for HMB-45, cathepsin K, and at least one muscle marker, with most expressing melan-A (77%) and/or MiTF (79%). A *PSF-TFE3* fusion was identified in one while another showed a *RAD51B-OPHN1* fusion. Follow-up ranged from two to 175 (mean 41) months, with 63% of patients alive and well, 20% dead of disease, 13% alive with disease, and 3% dead from other causes. In the latter, patients were 39 and 49 years old, one had tuberous sclerosis, while the other had pulmonary lymphangioleiomyomatosis. Both tumors expressed HMB-45, cathepsin K, and muscle markers, but lacked *TFE3* and *RAD51B* rearrangements. The two patients are currently alive and well. Application of gynecologic-specific criteria ($\geq$ 4 features required for malignancy: size $\geq$ 5 cm, high-grade atypia, mitoses > 1/50 high-power fields, necrosis, and lymphovascular invasion) for

predicting outcome misclassified 36% (4/11) of aggressive tumors; thus, a modified algorithm with a threshold of three of these features is recommended to classify a PEComa as malignant.

Key words: Perivascular Epithelioid Cell Tumor; PEComa; Uterus; Tuberous Sclerosis; Diagnostic Criteria; TFE3; RAD51B

INTRODUCTION

Uterine perivascular epithelioid cell neoplasms (PEComas) are rare tumors with approximately 100 cases reported in the English literature including five small series (consisting of 6, 6, 8, 11, and 13 tumors) [1-5]. PEComas have often been confused with smooth muscle tumors as they show overlapping morphological and immunohistochemical features. However, adequate diagnosis is crucial given the potential for targeted therapy with mTOR inhibitors when they behave in an adverse manner. While an algorithm specific to gynecologic PEComas has been proposed to classify those that are likely to behave aggressively when a minimum of four atypical features are present (size $\geq$ 5 cm, high-grade atypia, mitoses > 1/50 high-power fields (HPF), necrosis, and lymphovascular invasion) [3], experience is limited and diagnostic criteria based on a small number of tumors (n=16, 13 uterine) have not been corroborated.

Besides their association with *TSC1* and *TSC2* mutations, and those harboring *TFE3* rearrangements, little is known about the molecular phenotype of uterine PEComas. To our knowledge, only one comprehensive genomic study has been performed wherein 38 PEComas from varying anatomic locations (including 11 uterine) were evaluated [5]. This study identified *RAD51B* fusions in three uterine PEComas, a rearrangement not present at any other location. Herein we describe the morphology and immunoprofile of 32 uterine PEComas, identify possible

TFE3 and *RAD51B* rearrangements by fluorescence in-situ hybridization (FISH), and apply the gynecologic-specific algorithm to assess its validity/reproducibility.

MATERIAL AND METHODS

After approval by the institutional review board at the Massachusetts General Hospital, surgical pathology archives and consultation files of one of the authors (E.O.) were searched for uterine PEComas. Thirty-nine tumors were identified, but seven were excluded for various reasons, resulting in a cohort of 32 (one previously reported [6]). Age, history of tuberous sclerosis, recurrences, and date/status at last follow-up were obtained from medical records or consulting pathologist when available. Macroscopic features including tumor size, location, and gross description were recorded from the pathology reports.

Pathologic Examination:

A minimum of four hematoxylin and eosin slides (range 4 to 19) were examined per tumor unless the lesion was entirely submitted in less. Tumor border was classified as pushing, overtly or focally (invasion limited to one high-power (400X) field) infiltrative, or permeative (resembling endometrial stromal sarcoma). Architecture (sheets, nests, cords, trabeculae, fascicles, pseudoalveoli, single cells) and percentage of epithelioid and spindled cells were recorded. Nuclear atypia was graded as low (cells with little to no variation in size and shape), intermediate (up to two-fold variation) or high (greater than two-fold variation). Presence of multinucleated cells, Touton giant cells, 'melanoma-like' macronucleoli, intranuclear pseudoinclusions, and melanin pigment was noted, and cytoplasm was characterized as clear/eosinophilic and granular, rhabdoid, or foamy. Mitotic index per 10 and 50 HPFs, atypical mitoses, lymphovascular invasion, and necrosis were recorded when present. Degree of stromal

hyalinization (absent, focal, or diffuse), vessel morphology (thin and delicate, thin and ectatic, thick-walled, staghorn), and perivascular/radial distribution of tumor cells were also noted.

Immunohistochemistry:

Primary monoclonal antibodies to HMB-45 (clone HMB45, ready to use; Leica Biosystems, Buffalo Grove, IL), melan-A (clone A103, ready to use; Leica Biosystems), MiTF (clone C5/D5, ready to use; Bio SB, Santa Barbara, CA), cathepsin K (clone 3F9, ready to use; Cell Marque, Rocklin, CA), desmin (clone DE-R-11, ready to use; Leica Biosystems), smooth muscle actin (clone alpha sm-1, ready to use; Leica Biosystems), and h-caldesmon (clone h-CD ER1, dilution 1:100; Dako, Santa Clara, CA, USA) were applied to a representative 5 μm-thick section of formalin-fixed, paraffin-embedded tumor. Stains were interpreted as less than 1% expression (0), 1-5% (1+), 6-25% (2+), 26-50% (3+), and >50% (4+). Intensity was graded as strong, heterogeneous, or weak. Stains were considered positive if a nuclear (MiTF) or cytoplasmic (HMB-45, melan-A, cathepsin K, desmin, smooth muscle actin, h-caldesmon) pattern was noted.

Fluorescence In-Situ Hybridization:

FISH on interphase nuclei from paraffin-embedded 5 μm-thick sections was performed applying custom probes using bacterial artificial chromosomes (BAC), covering and flanking *TFE3* in Xp11.23 and *RAD51B* in 14q24.1. BAC clones were chosen according to the UCSC genome browser (http://genome.ucsc.edu) [5]. The BAC clones were obtained from BACPAC sources of Children's Hospital of Oakland Research Institute (Oakland, CA; http://bacpac.chori.org). DNA from individual BACs was isolated according to the manufacturer's instructions, labeled with different fluorochromes in a nick translation reaction, denatured, and hybridized to pretreated slides. Slides were then incubated, washed, and mounted

with DAPI in an antifade solution. The genomic location of each BAC set was verified by hybridizing them to normal metaphase chromosomes. Two hundred successive nuclei were examined using a Zeiss fluorescence microscope (Zeiss Axioplan, Oberkochen, Germany), controlled by Isis 5 software (Metasystems, Newton, MA). A positive score was interpreted when at least 20% of nuclei showed a break-apart signal. Nuclei with an incomplete set of signals were omitted from the score.

Statistical Analysis:

An adverse clinical course was defined as extrauterine disease, recurrence, and/or death. Associations between clinical outcome (benign versus aggressive) and pathological features were evaluated using Fisher's exact and Mann-Whitney U tests for categorical and continuous variables, respectively. To assess the performance of continuous variables in predicting adverse behavior, receiver-operator curves were built and the area under the curve and 95% confidence intervals were obtained. Sensitivity and specificity for different cutoff values was then calculated. Multivariate analyses were conducted using binomial logistic regression, obtaining odds ratios, and 95% confidence intervals. All hypothesis tests were two-sided and statistical significance was set at $p < 0.05$. Statistical analyses were performed using SAS software (version 9.4, SAS Institute, Cary, NC) and Stata (Version 14.0, StataCorp, College Station, TX).

RESULTS

CLASSIC APPEARANCE (n=30):

Clinical Features:

Patients ranged from 32 to 77 (mean 51.2, median 51.5) years and 13% (4/30) had a history of tuberous sclerosis. Clinical presentation was non-specific and included menorrhagia (33%, 10/30), pelvic/adnexal/uterine mass (17%, 5/30), presumed fibroids (17%, 5/30), pelvic

TABLE 1. Clinical Features of Patients With Aggressive Uterine PEComas

Case #	Age (y)	Clinical Presentation	Extrauterine Disease	Recurrences	Time to Recurrence (mo)	Status at Follow-Up	Follow-Up (mo)
1	63	Myometrial mass	None	Lung	12	DOD	43
3	50	Abdominal pain	Ovary	Mediastinum	7	AWD	7
4	63	Metrorrhagia	None	Omentum, small bowel and sigmoid fat, lymph node	65	NED	175
					91		
				Pouch of Douglas, mesocolon	151		
				Peritoneum, liver			
6	63	Lung tumors	Lung, rib	None	NA	DOD	5
8	48	Metastatic uterine sarcoma	Lungs	Vagina	8	DOD	18
9	64	Pelvic mass	Appendix, perirectal soft tissue, lymph nodes	Pelvis	5	AWD	24
				Liver	11		
10	67	Abdominal pain	None	Lung	19	DOD	20
11	62	Abnormal bleeding	None	Lung	44	AWD	66
				Lung	46		
				Liver/lung	65		
12	55	Unknown	Lungs	None	NA	DOD	6
13	53	Postmenopausal bleeding	None	Sacrum	2	AWD	29
31	59	Menorrhagia	None	Vagina	7	DOD	24
				Lungs	16		

AWD indicates alive with disease; DOD, dead of disease; NA, not applicable; NED, no evidence of disease.

pain (10%, 3/30), previously identified metastases from uterine primary (7%, 2/30), uterine prolapse (3%, 1/30), and cervical polyp (3%, 1/30). In the remaining 10% (3/30), presentation was not available. A total hysterectomy was performed in 80% (24/30), myomectomy in 7% (2/30), polypectomy in 7% (2/30), supracervical hysterectomy in 3% (1/30), and trachelectomy in 3% (1/30) of patients. Extrauterine disease was noted in 17% (5/30), with pulmonary metastases being most common (Table 1).

Pathologic Examination:

On gross examination, most tumors (77%, 23/30) arose in the corpus whereas the remaining 23% (7/30) were centered in the cervix. Tumors ranged from 0.2 to 17 (mean 5.5, median 4.3; size unavailable in two) cm. Their cut surface ranged from pink to tan-brown to yellow-brown to white and a subset were hemorrhagic (20%, 6/30) or necrotic (17%, 5/30) (Figure 1). A soft consistency was described in 17% (5/30) while another 17% (5/30) were firm and 10% (3/30) friable.

On microscopic evaluation, adjacent normal myometrium was present in 93% (28/30) of tumors allowing for evaluation of tumor-myometrium interface. A well-circumscribed, pushing border was noted in 18% (5/28) of tumors while invasion was present in 82% (23/28) (Figure 2). The latter more frequently had an infiltrative pattern (overt 52%, 12/23; focal 30%, 7/23), rarely a permeative growth (4%, 1/23), and three tumors (13%) showed a combined infiltrative/permeative pattern of invasion.

Tumors had one or more architectural patterns with nests being the most common (70%, 21/30), followed by sheets (60%, 18/30), trabeculae (30%, 9/30), cords (30%, 9/30), fascicles (10%, 3/30), single cells (7%, 2/30), and pseudoalveoli (3%, 1/30). Epithelioid cells were noted in all PEComas comprising 25 to 100% (mean 86%, median 100%) of an individual tumor.

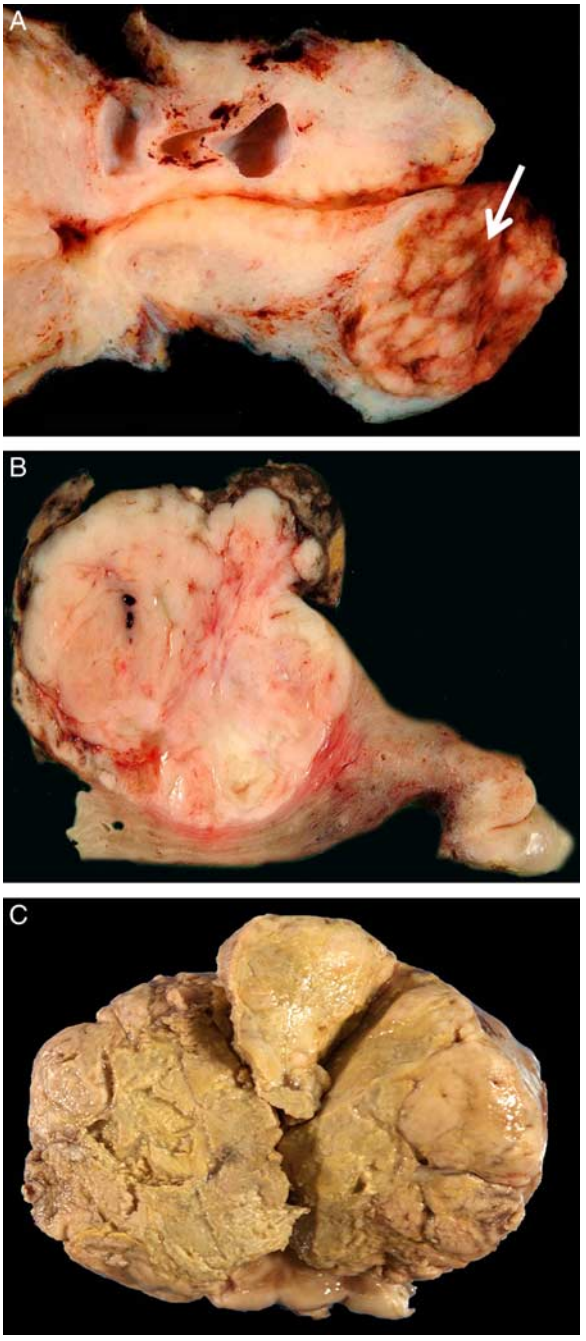

FIGURE 1. Uterine PEComas ranged from tan-pink and well-demarcated in the cervix (A, arrow) and corpus (B) to diffusely necrotic and infiltrative (C).

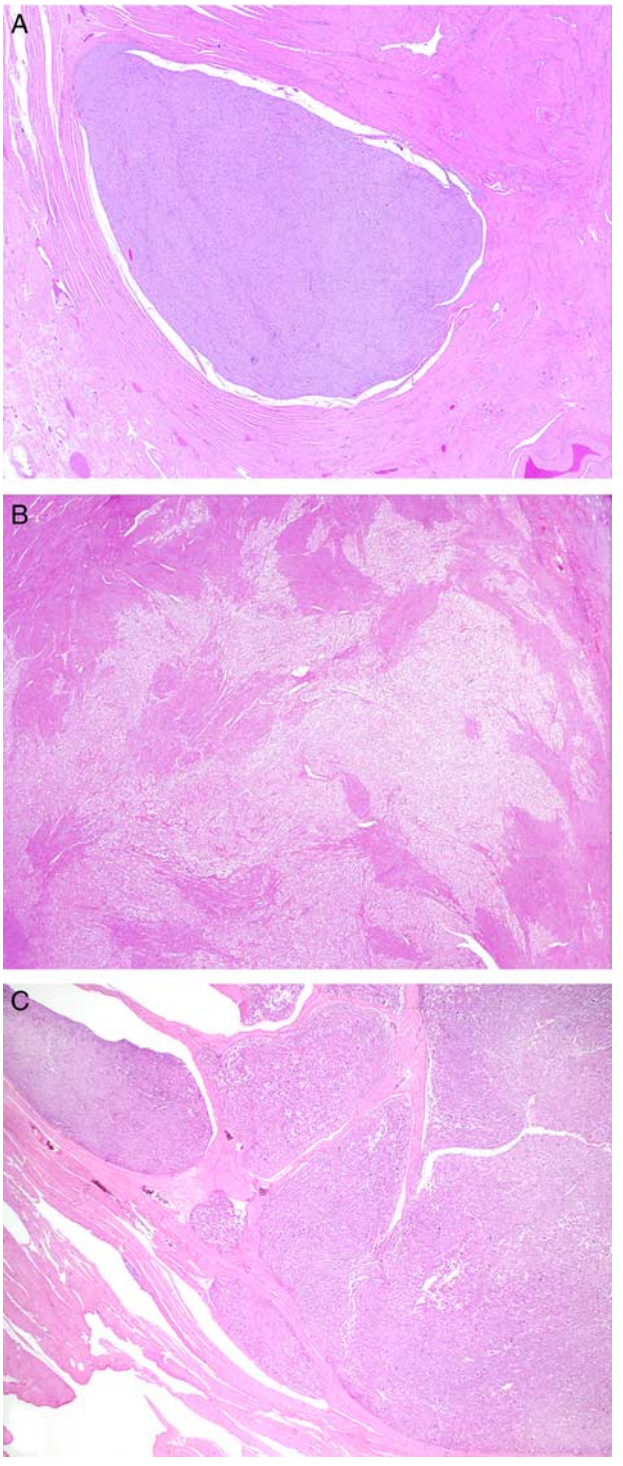

FIGURE 2. A well-circumscribed and pushing border was infrequent (A). Most PEComas were infiltrative (B) and a subset showed permeative growth (C).

Spindled cells were present in 37% (11/30) and ranged from 1 to 75% (mean 37%, median 30%). Nuclear atypia was low in 53% (16/30), intermediate in 17% (5/30), and high in 30% (9/30) (Figure 3A-3C). Most tumors (93%, 28/30) showed classic clear/eosinophilic and granular cytoplasm (Figure 3D), whereas the remaining 7% (2/30) had dense eosinophilic cytoplasm with a rhabdoid appearance. In those with typical cytoplasmic features, a rhabdoid appearance was focally observed in 43% (12/28) and a foamy appearance in 11% (3/28) (Figure 3E and 3F). 'Melanoma-like' macronucleoli were observed in 40% (12/30), multinucleated cells in 30% (9/30), intranuclear pseudoinclusions in 27% (8/30), Touton giant cells in 13% (4/30), and melanin pigment in 7% (2/30) (Figure 4A-4C). Mitoses ranged from 0 to 36 (mean 5.7, median 1) per 10 HPFs and from 0 to 133 (mean 19.2, median 2.5) per 50 HPFs, with atypical mitoses seen in 30%. Due to small tumor size or hypocellularity, 50 HPFs were not able to be evaluated in two tumors. Necrosis was noted in 30% (9/30) and lymphovascular invasion in 10% (3/30).

Stromal hyalinization was noted in 73% (22/30) of tumors (Figure 4D), being diffuse in one and diagnostic of sclerosing PEComa. Plaque-like hyalinization, similar to that seen in endometrial stromal sarcomas, was observed in 18% (4/22), and in one tumor, the stroma was focally myxoid. Thin and delicate vessels were present in all PEComas (Figure 4E), thin and ectatic vessels in 43% (13/30), thick-walled vessels in 37% (11/30), and staghorn vessels in 13% (4/30). Thick-walled vessels were more commonly (64%, 7/11) located at the periphery. A radial/perivascular distribution of tumor cells was observed in 23% (7/30) of neoplasms (Figure 4F).

A spindled smooth muscle-like phenotype was noted in 13% (4/30). The most striking example (case 11) consisted of long fascicles of spindled cells juxtaposed with atypical epithelioid cells (Figure 5A). Another tumor (case 8) was comprised of smooth muscle-like cells

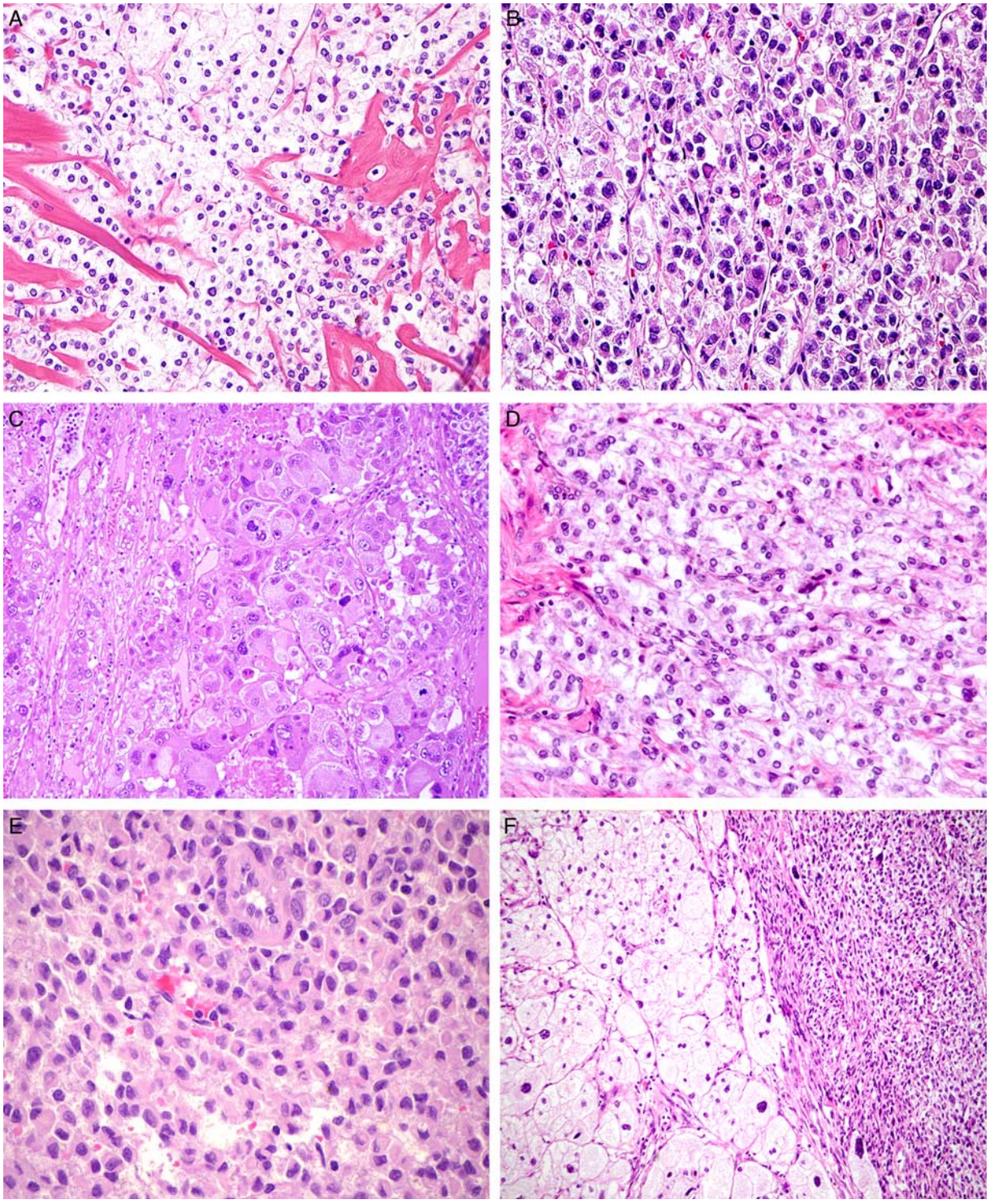

FIGURE 3. Cytologic atypia was low (A), intermediate (B), or high (C). Clear/eosinophilic and granular cytoplasm (D) was noted in most PEComas with a subset having a focal rhabdoid (E) or foamy (F) appearance.

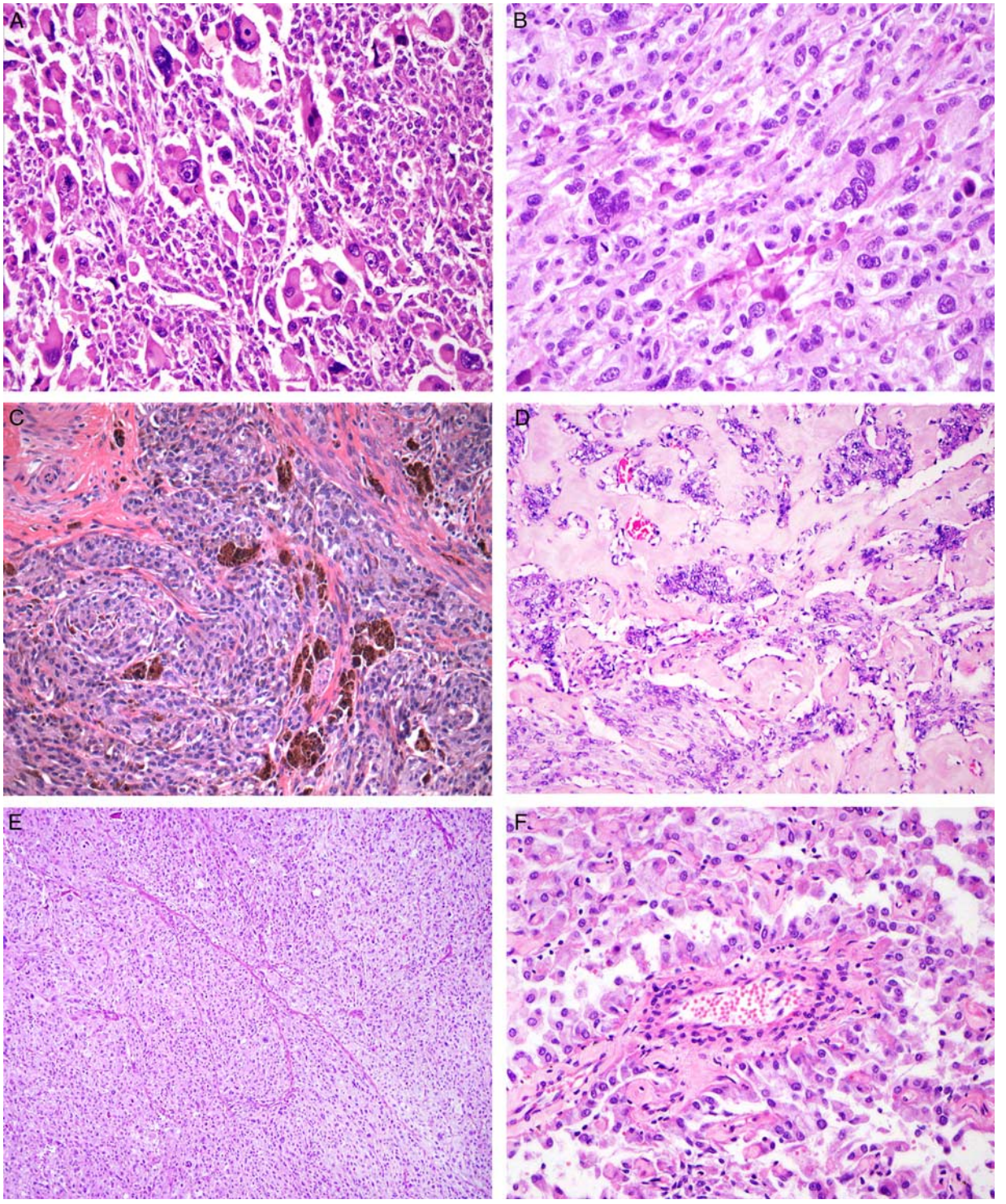

FIGURE 4. Other histologic features in uterine PEComas included "melanoma-like" macronucleoli (A), multinucleated cells (B), melanin pigment (C), and focal stromal hyalinization (D). Thin and delicate, capillary-like vasculature was a constant feature (E), but perivascular/radial distribution of cells (F) was only noted in a subset of tumors.

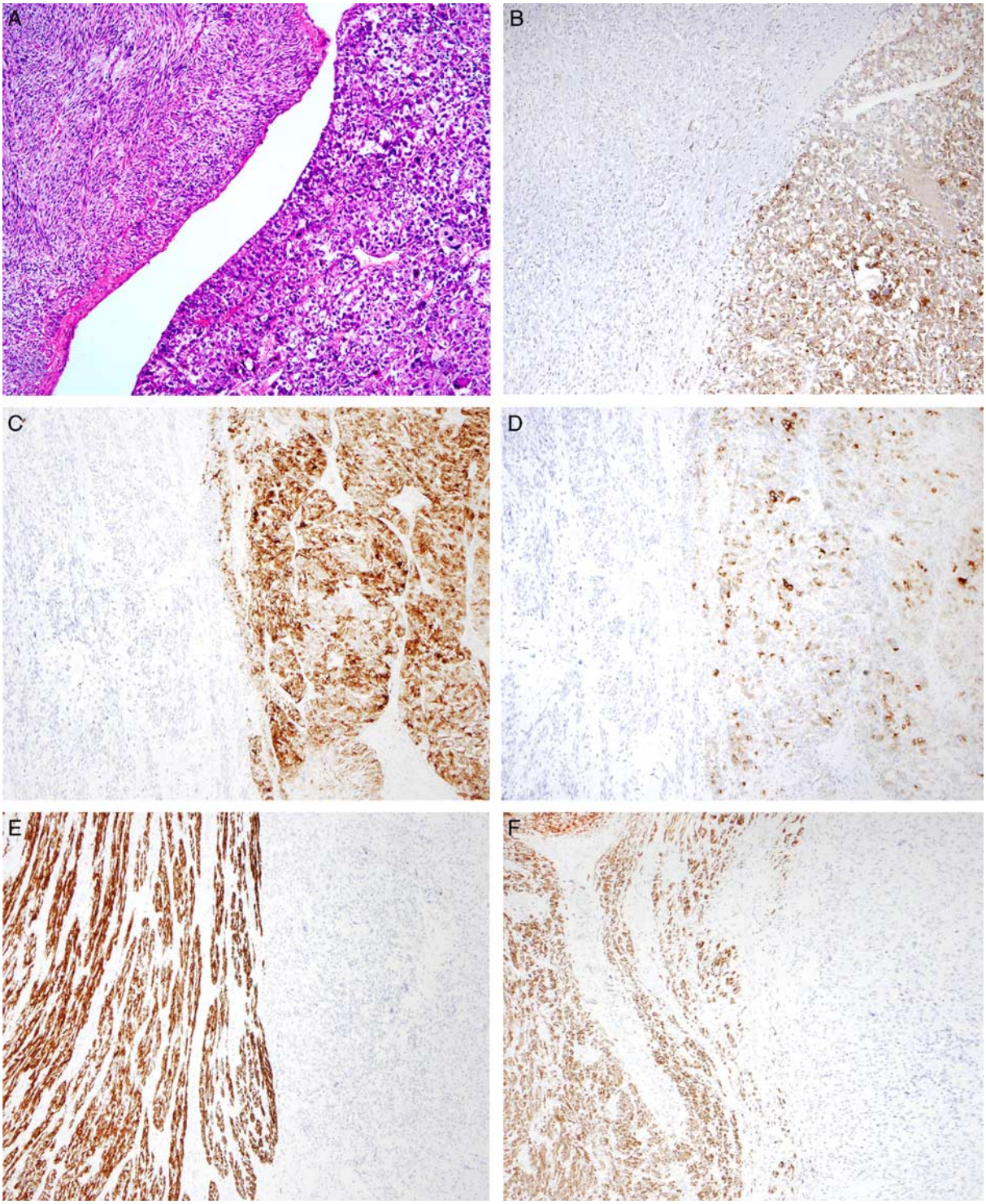

FIGURE 5. In case 11, spindled cells with striking smooth muscle-like differentiation (left) co-existed with epithelioid cells (right) (A). The epithelioid component (right) was strongly positive for cathepsin K (B), HMB-45 (C), and melan-A (D), but negative for desmin (E) and h-caldesmon (F). The inverse staining pattern was noted in the spindled component.

in a hyalinized background multifocally "infiltrated" by nests and cords of epithelioid cells. The third tumor (case 1) showed small irregular bundles of smooth muscle, histologically different from the uninvolved myometrium, scattered throughout the tumor. In the fourth (case 13), a rim of spindled cells with bizarre nuclei (resembling a leiomyoma with bizarre nuclei) was present between the main tumor mass and adjacent myometrium. Focal involvement of adenomyosis by tumor was seen in one tumor (case 16).

Immunohistochemistry:

Immunohistochemical results are summarized in Table 2. HMB-45 and cathepsin K were positive in all PEComas, with most showing 3+/4+ expression (83% and 93%, respectively). Melan-A and MiTF were expressed in 77% (23/30) and 79% (22/28) of tumors, but with variable intensity. Each PEComa was positive for at least one muscle marker, with smooth muscle actin being the most common (90%, 26/29), followed by desmin (22/29, 76%) and h-caldesmon (75%, 21/28), and all three showed variable intensity. In the tumor with a striking spindle smooth muscle-like component (case 11), the epithelioid cells were strongly positive for HMB-45, cathepsin K, and melan-A, but negative for desmin, h-caldesmon, and smooth muscle actin, while the spindled cells showed the opposite staining pattern (Figure 5B-5F). The spindled smooth muscle-like component in the other three PEComas was focal, and immunostains were not performed in these areas. In 75% (3/4) of tuberous sclerosis-associated PEComas (cases 2, 7, 16, 17), a similar immunoprofile was noted consisting of strong HMB-45 and cathepsin K expression, negative melan-A, and weak to negative MiTF. Besides the *TFE3*-rearranged PEComa (case 14, discussed below), only three other tumors (cases 25, 30, 26) were melan-A negative, but showed 3+/4+ MiTF expression.

Fluorescence In-Situ Hybridization:

FISH for *TFE3* and *RAD51B* rearrangements was successfully performed in 28 PEComas, with one showing a *PSF-TFE3* fusion and another having a *RAD51B-OPHN1* fusion (Figure 6, Table 2).

Follow-Up:

Follow-up was available for all patients and ranged from two to 175 (mean 41, median 20) months, with 63% (19/30) of patients alive and well, 20% (6/30) dead of disease, 13% (4/30) alive with disease, and 3% (1/30) dead from other causes. Recurrences occurred in 30% (9/30), with an average progression-free survival of 19 (range 2 to 65) months (Table 1). Of note, one patient (case 4) had three recurrences and as of last follow-up was alive without evidence of disease.

Statistical Analysis:

On univariate analysis, size $\geq$ 5 cm ($p < 0.001$), high-grade nuclear atypia ($p < 0.001$), necrosis ($p < 0.001$), mitoses > 1/50 HPFs ($p=0.002$), , and lymphovascular invasion ($p=0.041$), were associated with aggressive behavior. We sought to identify independent predictors of adverse behavior among the variables demonstrating statistically significant associations in univariate analyses. However, after conducting a binary logistic regression using stepwise selection ("enter" and "keep" thresholds of $p < 0.20$ and $p < 0.10$, respectively) we were not able to identify a single independent predictor.

LYMPHANGIOLEIOMYOMATOSIS APPEARANCE (n=2):

Clinical Features:

A 39 year-old patient (case 27) presented with lymphangioleiomyomatosis (LAM) in the lungs and imaging showed uterine and pelvic sidewall masses. The other patient was 49 years-

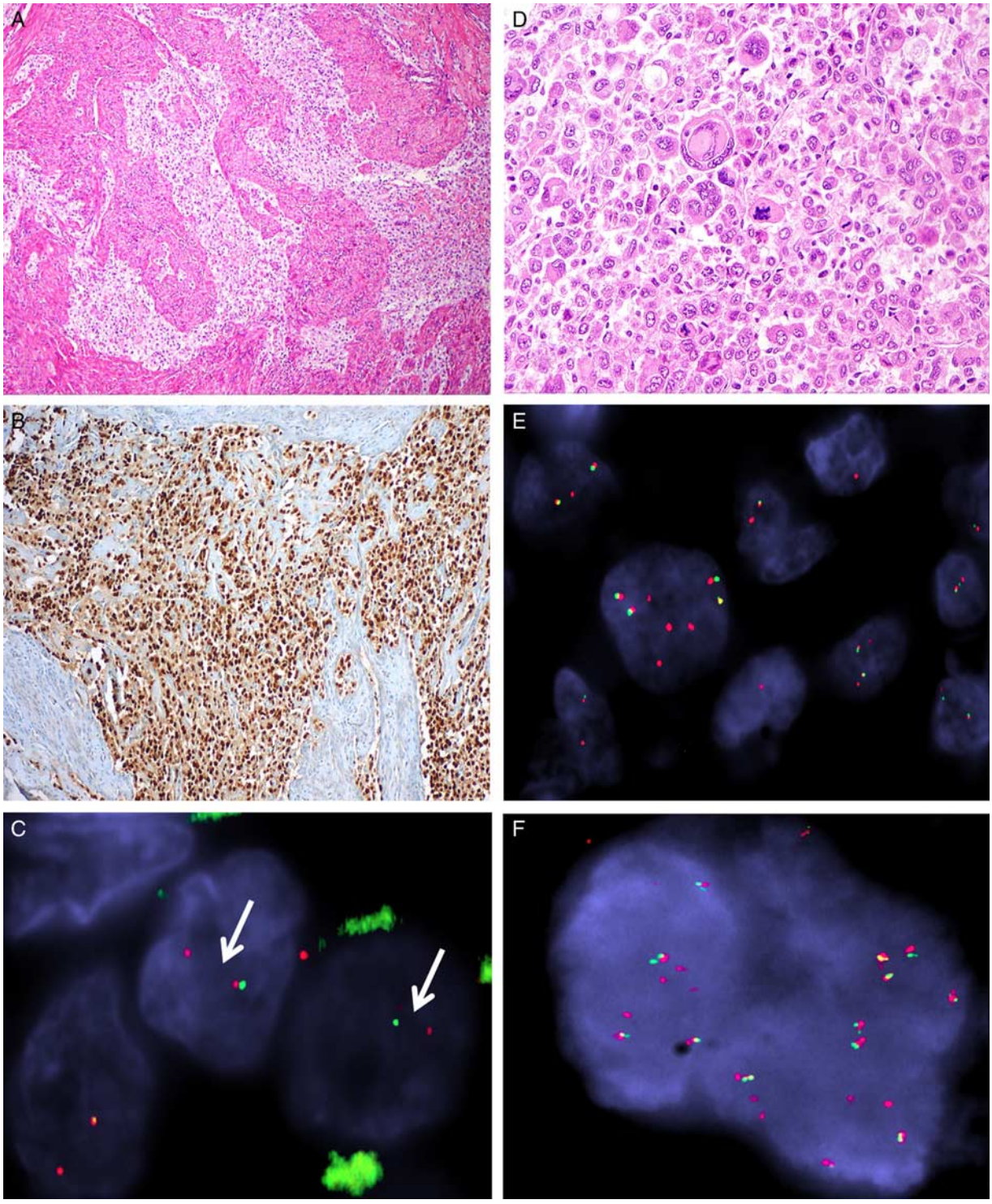

FIGURE 6. In case 14, epithelioid clear cells with alveolar and nested patterns (A) were strongly positive for TFE3 by immunohistochemistry (B) with *PSF* and *TFE3* rearrangements by FISH (C, arrows), as is typically seen in *TFE3*-rearranged PEComas. In case 12, diffuse sheets of highly atypical and mitotically active epithelioid cells (D) showed unbalanced complex *RAD51B* (E) and *OPHN1* (F) gene rearrangements by FISH.

TABLE 2. Immunohistochemical and Molecular Profile of Uterine PEComas

Case #	HMB-45	Melan-A	MiTF	Cathepsin K	Desmin	h-caldesmon	SMA	*TFE3*	*RAD51B*
1	4+ H	3+ S	2+ H	4+ S	0	1+	0	—	—
2	PPR	PPR	NP	NP	0	NP	PPR	NP	NP
3	3+ S	1+ S	1+ W	4+ S	1+ S	2+ H	2+ S	—	—
4	4+ S	4+ H	2+ W	4+ S	1+ W	3+ H	PPR	—	—
5	3+ H	PPR	NP	NP	NP	NP	4+ S	—	—
6	4+ S	1+ W	0	4+ S	0	1+ S	2+ S	—	—
7	3+ S	0	0	4+ S	4+ S	4+ S	3+ S	Failed	Failed
8	4+ S	3+ H	1+ W	4+ S	1+ S	1+ W	1+ H	—	—
9	4+ S	4+ S	0	4+ S	1+ H	2+ S	4+ S	—	—
10	3+ S	1+ W	1+ W	4+ S	3+ H	1+ S	1+ S	—	—
11	4+ S (Ep) 0 (Sp)	4+ S (Ep) 0 (Sp)	0 (Ep/Sp)	4+ S (Ep) 0 (Sp)	0 (Ep) 4+ (Sp)	0 (Ep) 4+ (Sp)	0 (Ep) 4+ (Sp)	—	—
12	2+ S	1+ S	2+ W	4+ S	2+ S	0	0	—	*RAD51B-OPHN1*
13	4+ S	2+ H	1+ W	4+ H	1+ S	0	NP	—	—
14	4+ S	0	0	4+ S	0	0	4+ S	*PSF-TFE3*	—
15	4+ S	3+ H	4+ S	4+ S	3+ S	0	2+ H	—	—
16	4+ S	0	1+ W	4+ S	4+ S	0	4+ S	—	—
17	4+ S	0	1+ W	4+ S	2+ S	0	PPR	—	—
18	4+ S	1+ H	3+ H	4+ S	4+ S	4+ S	4+ S	—	—
19	4+ S	4+ H	4+ W	4+ S	3+ S	2+ S	4+ H	—	—
20	1+ H	1+ S	3+ W	4+ S	2+ S	4+ S	4+ S	—	—
21	4+ S	4+ S	4+ S	2+ W	0	0	0	—	—
22	2+ S	2+ S	0	2+ H	4+ S	4+ S	3+ S	—	—
23	4+ S	1+ S	3+ W	4+ S	4+ S	4+ S	4+ S	—	—
24	2+ S	1+ H	4+ S	3+ S	4+ S	4+ S	4+ S	—	—
25	4+ H	0	4+ H	4+ S	4+ S	4+ S	4+ S	—	—
26	4+ S	0	3+ H	4+ S	4+ S	4+ S	4+ S	—	—
27	4+ S	0	0	4+ S	4+ S	4+ S	4+ S	—	—
28	4+ S	1+ W	2+ W	4+ H	0	4+ S	4+ S	—	—
29	4+ H	1+ W	3+ H	4+ S	4+ S	2+ S	4+ S	—	—
30	4+ S	0	4+ S	4+ S	4+ S	2+ S	4+ S	—	—
31	4+ S	4+ S	2+ H	4+ S	0	1+ H	2+ S	—	—
32	1+ S	1+ S	0	4+ S	4+ S	4+ S	4+ S	—	—

$<1\%$ (0), 1% to 5% (1+), 6% to 25% (2+), 26% to 50% (3+), $>50\%$ (4+), strong (S), heterogenous (H), weak (W).
Ep indicates epithelioid component; NP, not performed; PPR, positive per report; SMA, smooth muscle actin; Sp, spindled component.

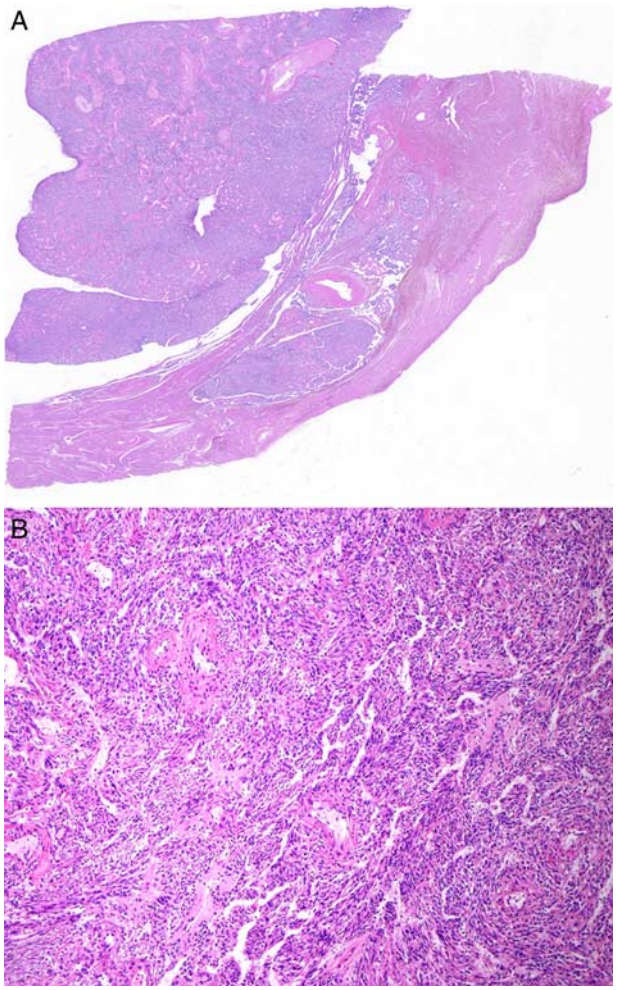

FIGURE 7. In case 27, a well-circumscribed mass was noted in the uterine wall (A) that had morphologic features characteristic of lymphangioleiomyomatosis (B).

TABLE 3. Classification of Uterine PEComas Using Nongynecologic Specific (Original) Criteria

		n/N (%)	
Classification	**Definition**	**PEComas With Aggressive Behavior Meeting Criteria**	**PEComas Without Aggressive Behavior Meeting Criteria***
Benign	< 5 cm, noninfiltrative, non-high-grade atypia, mitoses ≤ 1/50 HPFs, no necrosis, no LVI	0/0 (0)	1/19 (5)
Uncertain malignant potential	(1) Nuclear pleomorphism/multinucleated giant cells or (2) > 5 cm	0/0 (0)	1/19 (5)
Malignant	2+ features (> 5 cm, infiltrative, high-grade atypia, mitoses > 1/50 HPFs, necrosis, LVI)	11/11 (100)	6/19 (32)

*Eleven tumors without known malignancy could not be classified using the above criteria.
LVI indicates lymphovascular invasion.

old, had tuberous sclerosis, and presented with abnormal uterine bleeding (case 32). Both underwent total hysterectomy with extrauterine disease noted in one (retroperitoneum, case 27).

Pathological Examination:

Both tumors were located in the uterine corpus and measured 6 and 8 cm, respectively. On microscopic evaluation, one had an overtly infiltrative border (case 27) whereas the other merged with non-mass forming LAM (case 32). Both were comprised of low-grade spindled and epithelioid cells, thick-walled blood vessels, and cleft/slit-like spaces (Figure 7). Necrosis and mitoses were absent, but lymphovascular invasion was present in one (case 27).

Immunohistochemistry:

Case 27 showed strong and diffuse expression for HMB-45, cathepsin, desmin, h-caldesmon, and smooth muscle actin, but melan-A and MiTF were negative. Similarly, in case 32, cathepsin, desmin, h-caldesmon, and smooth muscle actin were strong and diffuse, but HMB-45 and MiTF were focal, and melan-A negative (Table 2).

Fluorescence In-Situ Hybridization:

TFE3 and *RAD51B* rearrangements were not identified.

Follow-Up:

The patient with pulmonary LAM (case 27) is alive with stable lung disease after 78 months. Neither patient has experienced a recurrence of their uterine PEComa.

DISCUSSION

Uterine PEComas were first reported in 2002 [1], but only two series have investigated whether the type and number of atypical pathologic features may predict clinical outcome [2, 3]. Herein we describe the morphological, immunohistochemical, and *TFE3/RAD51B* fusion status of the largest series of uterine PEComas to date and evaluate algorithms to predict outcome in

these tumors. The original PEComa classification developed by Folpe et al. categorized tumors as either benign (no atypical features), uncertain malignant potential (nuclear pleomorphism/multinucleated giant cells or size > 5 cm), or malignant (two or more of the following: size > 5 cm, infiltrative growth, high nuclear grade and cellularity, mitoses > 1/50 HPFs, necrosis, and lymphovascular invasion) [2]. Using this algorithm for their series of 16 gynecologic PEComas, Schoolmeester et al. noted that all aggressive PEComas were classified as malignant, but 57% of benign PEComas were also classified as malignant, and three tumors did not fulfill criteria to be assigned a category [3]. Thus, they proposed a modified gynecologic-specific algorithm based upon five statistically significant features (size $\geq$ 5 cm, high-grade atypia (excluding degenerative atypia), mitoses > 1/50 HPFs, necrosis, and lymphovascular invasion) with the presence of at least four features required to make a diagnosis of malignant PEComa. In addition, they reduced the number of categories to two—benign/uncertain malignant potential and malignant. Using this algorithm, their 16 PEComas were accurately classified.

Application of the original algorithm in our series showed an analogous trend with all aggressive PEComas classified as malignant. However, 37% (7/19) of benign tumors were misclassified, and 37% (11/30) did not fulfill criteria for any category (Table 3). When the gynecologic-specific algorithm was applied, 36% (4/11) of aggressive PEComas were incorrectly classified (Table 4). Three of the four misclassified PEComas (cases 1, 12, 31) had three atypical pathologic features, whereas those with a favorable outcome had a maximum of two (Table 5). When reviewing the series by Schoolmeester and colleagues, only one tumor (case 3) had three worrisome features, but it behaved in a benign fashion, with their remaining benign PEComas exhibiting up to two atypical features [3]. Follow-up, however, was relatively

brief (27 months), and given that two of our tumors did not recur until 44 and 65 months after initial diagnosis, it is possible that this PEComa may ultimately have recurred. Furthermore, this tumor measured 5 cm, which just met the size cutoff to be considered an atypical feature.

When the gynecologic-specific algorithm described by Schoolmeester and colleagues [3] was applied to the six uterine PEComas reported by Folpe et al. one had three worrisome features and also behaved aggressively, whereas the remaining five were correctly classified [2]. Thus, we propose a threshold of three (as opposed to four) atypical features to diagnose a PEComa as malignant. Using this algorithm, all aggressive PEComas in this study, as well as those by Folpe et al. [2] are properly classified, and only one from Schoolmeester et al. [3] is misclassified.

The fourth aggressive PEComa in our series (case 4) that was classified as benign/uncertain malignant potential only had one atypical feature, a size of 5 cm. This tumor was quite peculiar in that the first recurrence occurred 65 months after diagnosis, followed by two additional recurrences at 91 and 151 months. While it is unknown whether the patient received any therapy besides surgery, she currently is alive without disease. This case exemplifies, as occurs in smooth muscle tumors, the fact that some of these PEComas, even when histologically benign, may rarely pursue an aggressive behavior. Therefore, we propose eliminating the term "benign" from the benign/uncertain malignant potential category.

The distinction of PEComa from a smooth muscle tumor in the uterus still remains a diagnostic challenge. One of the key morphological features we have observed to aid in favoring a diagnosis of PEComa is the presence of a delicate, capillary-like vasculature surrounding tumor cells and nests, a feature not characteristic of smooth muscle tumors. Conversely, thick-walled blood vessels are ubiquitous in leiomyomas, and while they might be seen in PEComas, they

typically are less numerous and often peripherally located. Additional features that favor the diagnosis of smooth muscle tumor include perinuclear vacuoles and diffuse eosinophilic cytoplasm without prominent cytoplasmic granularity [7].

In some tumors, morphology alone may be insufficient to distinguish PEComa from a smooth muscle tumor. Schoolmeester and colleagues proposed that in the appropriate morphological context (not described), focal staining by two melanocytic immunostains (preferably HMB-45 and melan-A) along with expression of at least one muscle marker is necessary to make the diagnosis of PEComa [3]. However, 44% (7/16) of their cases show $\leq$ 5% expression for both HMB-45 and melan-A. On the other hand, focal and occasionally diffuse expression for HMB-45 and/or melan-A has been reported in a subset of uterine smooth muscle tumors [8-16]. While MiTF was positive in 79% of our tumors, previous reports have noted its low sensitivity and specificity [2, 7], and in the absence of other melanocytic markers, we do not believe MiTF positivity alone justifies the diagnosis of PEComa.

Cathepsin K is a protease involved in osteoclast function that is regulated by the MiTF family [17] and is expressed in PEComas of the kidney [18] as well as extrarenal PEComas [19], but its expression in smooth muscle tumors is largely unknown. To our knowledge, it has only been evaluated in three series (uterine leiomyomas, uterine leiomyosarcomas, and leiomyosarcomas not specified) [16, 19, 20]. While all uterine leiomyomas were cathepsin K negative, 83% (25/30) of uterine leiomyosarcomas and 67% (8/12) of unspecified leiomyosarcomas showed at least focal staining. To further assess its expression in uterine leiomyosarcomas, we stained 20 of such tumors and found 4+ staining in 5% (1/20), 3+ in 35% (7/20), 2+ in 5% (1/20), 1+ in 30% (6/20), and 0 in 25% (5/20), all with weak or heterogeneous intensity (personal observation). Nonetheless, additional studies investigating cathepsin K

expression in uterine smooth muscle tumors are merited to determine its value as a diagnostic marker for uterine PEComas.

Originally, myoid markers (especially desmin) were considered to be more strongly expressed in tumors with a predominant spindled component and low numbers of clear cells [1, 7]. More recently, however, strong and diffuse desmin and h-caldesmon have been reported in a large cohort of PEComas [3], irrespective of the number of clear cells or percentage of spindled component. Similar findings were noted herein. Other markers that have been occasionally expressed in uterine PEComas include hormone receptors, pan-cytokeratins, S-100, tyrosinase, CD10, CD1a, CD117, and vimentin [1-3, 7, 21], but none have proved to be of diagnostic value in differentiating between a PEComa and smooth muscle tumor.

Smooth muscle-like differentiation in PEComas has only been briefly mentioned in the literature, but was noted in four of our cases. In the most striking example, the epithelioid and spindled morphologies were juxtaposed and had completely opposite staining patterns. The epithelioid component expressed melanocytic markers while the spindled foci, which histologically resembled a smooth muscle neoplasm rather than a spindled PEComa, were positive for muscle markers. This observation contrasts that reported by Folpe et al. who noted that none of their desmin-positive PEComas showed the previously described morphologic features compatible with smooth muscle tumors [2, 7]. However, Choi et al. described a somewhat similar lesion that consisted of ovoid to spindled cells infiltrating what appeared to be a leiomyoma [22]. The infiltrative neoplasm was positive for HMB-45, smooth muscle actin, and TFE3, but negative for desmin and h-caldesmon, while the presumed leiomyoma showed the opposite pattern of staining. The question of whether these lesions represent a collision between

a PEComa and smooth muscle tumor versus a PEComa with smooth muscle differentiation remains unknown, but perhaps may be answered by molecular analysis.

A subset of PEComas has shown *TFE3* rearrangements. Testing immunohistochemical TFE3 expression can be challenging as the protein is ubiquitously present in low levels in normal cells. As a result, the antibody often shows low specificity, which may be improved via a manual preparation with overnight incubation [23]. For this reason, we evaluated for *TFE3* translocations upfront by FISH. A *PSF-TFE3* fusion was identified in one tumor and to our knowledge, only one other *PSF-TFE3* rearranged PEComa of the gynecological tract has been reported, which was of cervical origin [24, 25]. Regardless of site and fusion partner, most *TFE3*-associated PEComas show similar morphologic features including alveolar or nested growth, predominant epithelioid component, low nuclear atypia, and rare mitoses [4, 5, 26], all of which were characteristic of the tumor herein. Strong expression of HMB-45 and TFE3, focal or absent melan-A and smooth muscle markers, and negative MiTF is also typical of these tumors [4, 5, 26]. With the exception of diffuse expression of smooth muscle actin, this immunoprofile matched our current case. Of the 32 reported extrarenal *TFE3*-associated PEComas [4, 5, 24-35], follow-up was available in 72% (23/32), 52% (12/23) of which demonstrated aggressive behavior. The clinical course of our patient with the *TFE3*-associated PEComa has been uneventful; however, follow-up is relatively brief (19 months).

A different tumor showed a *RAD51B-OPHN1* rearrangement, which has only been described in three PEComas, all from the uterine corpus [5]. In the previous series, no distinct morphology was noted among the three tumors, but all showed brisk mitotic activity (> 10 per 10 HPFs) and positivity for HMB-45, smooth muscle actin, and desmin. Recurrences occurred in all three, one of which ultimately died of disease. Our *RAD51B*-rearranged PEComa also had an

elevated mitotic index (28 per 10 HPFs) and expressed HMB-45 and desmin, but was negative for smooth muscle actin. While she did not experience any recurrences, she initially presented with lung metastases and succumbed to disease after six months. Although the cohort of *RAD51B*-rearranged PEComas is small, preliminary data suggests this fusion is associated with aggressive behavior, but additional studies need to be performed to corroborate this observation. As a caveat, a subset of uterine smooth muscle tumors have been reported to show *RAD51B* mutations [36-41] thereby emphasizing the importance of strong expression for melanocytic markers, and if needed, molecular testing for *TSC* mutations, in the diagnostic work-up.

Finally, one unusual feature we noted in this series was the presence of two tumors having a LAM-like morphology. In the uterus, LAM is usually an incidental finding [6, 42-48], but occasionally presents as a discrete mass [45, 48-52]. Such patients typically have a history of tuberous sclerosis and/or pulmonary LAM, and undergo hysterectomy due to abnormal uterine bleeding, endometrial carcinoma, or an adnexal mass. Our two patients were no exception as one was previously diagnosed with pulmonary LAM and the other with tuberous sclerosis. The typical LAM morphology is generally sufficient to make the diagnosis, but when in doubt, HMB-45 and myoid markers may be helpful. While LAM often shows strong and diffuse desmin and smooth muscle actin, it is important to note that HMB-45 may be weak and patchy, or even negative, confounding the diagnosis [47, 53]. Similarly, melan-A can be negative or weak and patchy [47]. However, in both tumors in this study, as well as those from a recent series on pulmonary LAM [54], cathepsin K has been shown to be diffusely positive, even in the absence of HMB-45 staining.

In summary, we have described the largest series of uterine PEComas to date highlighting their wide morphologic spectrum, common expression of HMB-45 and cathepsin K, and

infrequent *TFE3* and *RAD51B* rearrangements. We propose two modifications to the current gynecologic-specific algorithm, which include elimination of the term "benign" in the benign/uncertain malignant potential category, and reduction of the number of features required for a diagnosis of malignancy to three. Both changes appear to more accurately classify these unique tumors.

ACKNOWLEDGEMENTS

We want to thank Drs. Alice Parisi (University and Hospital Trust of Verona, Verona, Italy), Esperanza Villanueva-Siles (Montefiore Medical Center, Bronx, NY, USA), Sachiko Minamiguchi (formerly at Kyoto Medical Center, Kyoto, Japan), Jacqueline Haas (Clinical Pathology Laboratories, Austin, TX, USA), Yukihiro Imai (Kobe City Medical Center General Hospital, Kobe, Japan), Teresa Alvarez (Institut Universitaire de Pathologie, Lausanne, Switzerland), Joana Loureiro and Carla Bartosch (Instituto Portugues de Oncologia, Porto, Portugual), Sophie Diebold-Berger (Viollier Weintraub SA, Geneva, Switzerland), Mohammed Nazed (The Christ Hospital, Cincinnati, OH, USA), Michael Jones and Emily Meserve (Maine Medical Center, Portland, ME, USA), and Nathan Johnston (Summit Pathology, Colorado Springs, CO, USA) for their contribution of cases.

REFERENCES

1. Vang R, Kempson RL. Perivascular epithelioid cell tumor ('PEComa') of the uterus: a subset of HMB-45-positive epithelioid mesenchymal neoplasms with an uncertain relationship to pure smooth muscle tumors. *Am J Surg Pathol.* 2002;26:1-13.

2. Folpe AL, Mentzel T, Lehr HA, et al. Perivascular epithelioid cell neoplasms of soft tissue and gynecologic origin: a clinicopathologic study of 26 cases and review of the literature. *Am J Surg Pathol.* 2005;29:1558-1575.

3. Schoolmeester JK, Howitt BE, Hirsch MS, et al. Perivascular epithelioid cell neoplasm (PEComa) of the gynecologic tract: clinicopathologic and immunohistochemical characterization of 16 cases. *Am J Surg Pathol.* 2014;38:176-188.

4. Schoolmeester JK, Dao LN, Sukov WR, et al. TFE3 translocation-associated perivascular epithelioid cell neoplasm (PEComa) of the gynecologic tract: morphology, immunophenotype, differential diagnosis. *Am J Surg Pathol.* 2015;39:394-404.

5. Agaram NP, Sung YS, Zhang L, et al. Dichotomy of Genetic Abnormalities in PEComas With Therapeutic Implications. *Am J Surg Pathol.* 2015;39:813-825.

6. Lim GS, Oliva E. The morphologic spectrum of uterine PEC-cell associated tumors in a patient with tuberous sclerosis. *Int J Gynecol Pathol.* 2011;30:121-128.

7. Folpe AL, Kwiatkowski DJ. Perivascular epithelioid cell neoplasms: pathology and pathogenesis. *Hum Pathol.* 2010;41:1-15.

8. Zamecnik M, Michal M. HMB45+ hyalinized epithelioid tumor of the uterus is linked to epithelioid leiomyoma rather than to PEC-omas. *Int J Surg Pathol.* 2001;9:341-343.

9. Silva EG, Deavers MT, Bodurka DC, et al. Uterine epithelioid leiomyosarcomas with clear cells: reactivity with HMB-45 and the concept of PEComa. *Am J Surg Pathol.* 2004;28:244-249.

10. Hurrell DP, McCluggage WG. Uterine leiomyosarcoma with HMB45+ clear cell areas: report of two cases. *Histopathology.* 2005;47:540-542.

11. Zamecnik M, Voltr L, Chlumska A. HMB45+ cells in mixed stromal-smooth muscle tumour of the uterus. *Histopathology.* 2006;48:463-464.

12. Michal M, Zamecnik M. Hyalinized Uterine Mesenchymal Neoplasms with HMB-45-Positive Epithelioid Cells: Epithelioid Leiomyomas or Angiomyolipomas? Report of Four Cases. *Int J Surg Pathol.* 2000;8:323-328.

13. Simpson KW, Albores-Saavedra J. HMB-45 reactivity in conventional uterine leiomyosarcomas. *Am J Surg Pathol.* 2007;31:95-98.

14. Oliva E, Wang WL, Branton P, et al. Expression of Melanocytic ("PEComa") Markers in Smooth Muscle Tumors of the Uterus: An Immunohistochemical Analysis of 86 Cases. *Mod Pathol.* 2006;19:191A.

15. Toyoshima M, Okamura C, Niikura H, et al. Epithelioid leiomyosarcoma of the uterine cervix: a case report and review of the literature. *Gynecol Oncol.* 2005;97:957-960.

16. Howitt BE, Schoolmeester JK, Quade BJ, et al. Immunohistochemical Analysis of HMB-45, MelanA and Cathepsin K in a Series of 35 Uterine Leiomyosarcoma. *Mod Pathol.* 2013;26:279A.

17. Motyckova G, Weilbaecher KN, Horstmann M, et al. Linking osteopetrosis and pycnodysostosis: regulation of cathepsin K expression by the microphthalmia transcription factor family. *Proc Natl Acad Sci U S A.* 2001;98:5798-5803.

18. Martignoni G, Pea M, Gobbo S, et al. Cathepsin-K immunoreactivity distinguishes MiTF/TFE family renal translocation carcinomas from other renal carcinomas. *Mod Pathol.* 2009;22:1016-1022.

19. Rao Q, Cheng L, Xia QY, et al. Cathepsin K expression in a wide spectrum of perivascular epithelioid cell neoplasms (PEComas): a clinicopathological study emphasizing extrarenal PEComas. *Histopathology.* 2013;62:642-650.

20. Zheng G, Martignoni G, Antonescu C, et al. A broad survey of cathepsin K immunoreactivity in human neoplasms. *Am J Clin Pathol.* 2013;139:151-159.

21. D'Angelo E, Prat J. Diagnostic use of immunohistochemistry in uterine mesenchymal tumors. *Semin Diagn Pathol.* 2014;31:216-222.

22. Choi YJ, Hong JH, Kim A, et al. A Case of Malignant PEComa of the Uterus Associated with Intramural Leiomyoma and Endometrial Carcinoma. *J Pathol Transl Med.* 2016;50:469-473.

23. Argani P, Lal P, Hutchinson B, et al. Aberrant nuclear immunoreactivity for TFE3 in neoplasms with TFE3 gene fusions: a sensitive and specific immunohistochemical assay. *Am J Surg Pathol.* 2003;27:750-761.

24. Rao Q, Shen Q, Xia QY, et al. PSF/SFPQ is a very common gene fusion partner in TFE3 rearrangement-associated perivascular epithelioid cell tumors (PEComas) and melanotic Xp11 translocation renal cancers: clinicopathologic, immunohistochemical, and molecular characteristics suggesting classification as a distinct entity. *Am J Surg Pathol.* 2015;39:1181-1196.

25. Liu F, Zhang R, Wang ZY, et al. Malignant perivascular epithelioid cell tumor (PEComa) of cervix with TFE3 gene rearrangement: a case report. *Int J Clin Exp Pathol.* 2014;7:6409-6414.

26. Argani P, Aulmann S, Illei PB, et al. A distinctive subset of PEComas harbors TFE3 gene fusions. *Am J Surg Pathol.* 2010;34:1395-1406.

27. Williamson SR, Bunde PJ, Montironi R, et al. Malignant perivascular epithelioid cell neoplasm (PEComa) of the urinary bladder with TFE3 gene rearrangement: clinicopathologic, immunohistochemical, and molecular features. *Am J Surg Pathol.* 2013;37:1619-1626.

28. Shen Q, Rao Q, Xia QY, et al. Perivascular epithelioid cell tumor (PEComa) with TFE3 gene rearrangement: clinicopathological, immunohistochemical, and molecular features. *Virchows Arch.* 2014;465:607-613.

29. Tanaka M, Kato K, Gomi K, et al. Perivascular epithelioid cell tumor with SFPQ/PSF-TFE3 gene fusion in a patient with advanced neuroblastoma. *Am J Surg Pathol.* 2009;33:1416-1420.

30. Hyrcza MD, Winer DA, Shago M, et al. TFE3-Expressing Perivascular Epithelioid Cell Neoplasm (PEComa) of the Sella Turcica. *Endocr Pathol.* 2017;28:22-26.

31. Shon W, Kim J, Sukov W, et al. Malignant TFE3-rearranged perivascular epithelioid cell neoplasm (PEComa) presenting as a subcutaneous mass. *Br J Dermatol.* 2016;174:617-620.

32. Lu B, Wang C, Zhang J, et al. Perivascular epithelioid cell tumor of gastrointestinal tract: case report and review of the literature. *Medicine (Baltimore).* 2015;94:e393.

33. Lee SE, Choi YL, Cho J, et al. Ovarian perivascular epithelioid cell tumor not otherwise specified with transcription factor E3 gene rearrangement: a case report and review of the literature. *Hum Pathol.* 2012;43:1126-1130.

34. Russell CM, Buethe DD, Dickinson S, et al. Perivascular epithelioid cell tumor (PEComa) of the urinary bladder associated with Xp11 translocation. *Ann Clin Lab Sci.* 2014;44:91-98.

35. LeGallo RD, Stelow EB, Sukov WR, et al. Melanotic xp11.2 neoplasm of the ovary: report of a unique case. *Am J Surg Pathol.* 2012;36:1410-1414.

36. Mehine M, Kaasinen E, Heinonen HR, et al. Integrated data analysis reveals uterine leiomyoma subtypes with distinct driver pathways and biomarkers. *Proc Natl Acad Sci U S A.* 2016;113:1315-1320.

37. Schoenmakers EF, Huysmans C, Van de Ven WJ. Allelic knockout of novel splice variants of human recombination repair gene RAD51B in t(12;14) uterine leiomyomas. *Cancer Res.* 1999;59:19-23.

38. Kampjarvi K, Park MJ, Mehine M, et al. Mutations in Exon 1 highlight the role of MED12 in uterine leiomyomas. *Hum Mutat.* 2014;35:1136-1141.

39. Pradhan B, Sarvilinna N, Matilainen J, et al. Detection and screening of chromosomal rearrangements in uterine leiomyomas by long-distance inverse PCR. *Genes Chromosomes Cancer.* 2016;55:215-226.

40. Thibodeau ML, Reisle C, Zhao E, et al. Genomic profiling of pelvic genital type leiomyosarcoma in a woman with a germline CHEK2:c.1100delC mutation and a concomitant diagnosis of metastatic invasive ductal breast carcinoma. *Cold Spring Harb Mol Case Stud.* 2017;3.

41. Mehine M, Kaasinen E, Makinen N, et al. Characterization of uterine leiomyomas by whole-genome sequencing. *N Engl J Med.* 2013;369:43-53.

42. Lack EE, Dolan MF, Finisio J, et al. Pulmonary and extrapulmonary lymphangioleiomyomatosis. Report of a case with bilateral renal angiomyolipomas, multifocal lymphangioleiomyomatosis, and a glial polyp of the endocervix. *Am J Surg Pathol.* 1986;10:650-657.

43. Gyure KA, Hart WR, Kennedy AW. Lymphangiomyomatosis of the uterus associated with tuberous sclerosis and malignant neoplasia of the female genital tract: a report of two cases. *Int J Gynecol Pathol.* 1995;14:344-351.

44. Sato T, Seyama K, Kumasaka T, et al. A patient with TSC1 germline mutation whose clinical phenotype was limited to lymphangioleiomyomatosis. *J Intern Med.* 2004;256:166-173.

45. Torres VE, Bjornsson J, King BF, et al. Extrapulmonary lymphangioleiomyomatosis and lymphangiomatous cysts in tuberous sclerosis complex. *Mayo Clin Proc.* 1995;70:641-648.

46. Clay MR, Gibson P, Lowell J, et al. Microscopic uterine lymphangioleiomyomatosis perivascular epithelioid cell neoplasm: a case report with the earliest manifestation of this enigmatic neoplasm. *Int J Gynecol Pathol.* 2011;30:71-75.

47. Rabban JT, Firetag B, Sangoi AR, et al. Incidental Pelvic and Para-aortic Lymph Node Lymphangioleiomyomatosis Detected During Surgical Staging of Pelvic Cancer in Women Without Symptomatic Pulmonary Lymphangioleiomyomatosis or Tuberous Sclerosis Complex. *Am J Surg Pathol.* 2015;39:1015-1025.

48. Hayashi T, Kumasaka T, Mitani K, et al. Prevalence of uterine and adnexal involvement in pulmonary lymphangioleiomyomatosis: a clinicopathologic study of 10 patients. *Am J Surg Pathol.* 2011;35:1776-1785.

49. Longacre TA, Hendrickson MR, Kapp DS, et al. Lymphangioleiomyomatosis of the uterus simulating high-stage endometrial stromal sarcoma. *Gynecol Oncol.* 1996;63:404-410.

50. Han JM, Lee KH, Kim SJ, et al. A case of lymphangioleiomyomatosis originated in the pelvic cavity. *J Gynecol Oncol.* 2008;19:195-198.

51. Kim YS, Rha SE, Byun JY, et al. CT and MR imaging findings of lymphangioleiomyomatosis involving the uterus and pelvic cavity. *Korean J Radiol.* 2011;12:261-265.

52. Szpurek D, Szubert S, Zielinski P, et al. Malignant presentation of uterine lymphangioleiomyomatosis. *Taiwan J Obstet Gynecol.* 2015;54:603-607.

53. Schoolmeester JK, Park KJ. Incidental Nodal Lymphangioleiomyomatosis Is Not a Harbinger of Pulmonary Lymphangioleiomyomatosis: A Study of 19 Cases With Evaluation of Diagnostic Immunohistochemistry. *Am J Surg Pathol.* 2015;39:1404-1410.

54. I. R, Makupsorr MS, Lovrenski A, et al. A Comparison of Antibodies HMB-45 and Cathepsin-K as Diagnostic Markers of Pulmonary Lymphangioleiomyomatosis. *Mod Pathol.* 2018;31:748.